

Supporting Information

LDH-derived $\text{Co}_{0.5}\text{Ni}_{0.5}\text{Te}_2$ Dispersed in 3D Carbon Sheets as Separator Modifier to Enable Kinetics-Accelerated Lithium-Sulfur Batteries

Chunmei Li,^{a,b} Kan Mi,^{*a,b} Kai Xu,^a Zhusuo Jia,^a Xiaolei Jiang,^{a,b} Huili Peng,^{a,b} Xiuwen Zheng^{*b,c} and Hongjiao Nie^{*a,b}

^a School of Chemistry and Chemical Engineering, Linyi University, Linyi, 276000, China

E-mail: mikan@lyu.edu.cn, niehongjiao@lyu.edu.cn

^b Key Laboratory of Advanced Biomaterials and Nanomedicine in Universities of Shandong, Linyi University, Linyi 276000, PR China

^c Qilu Normal University, Jinan, 250013, P. R. China

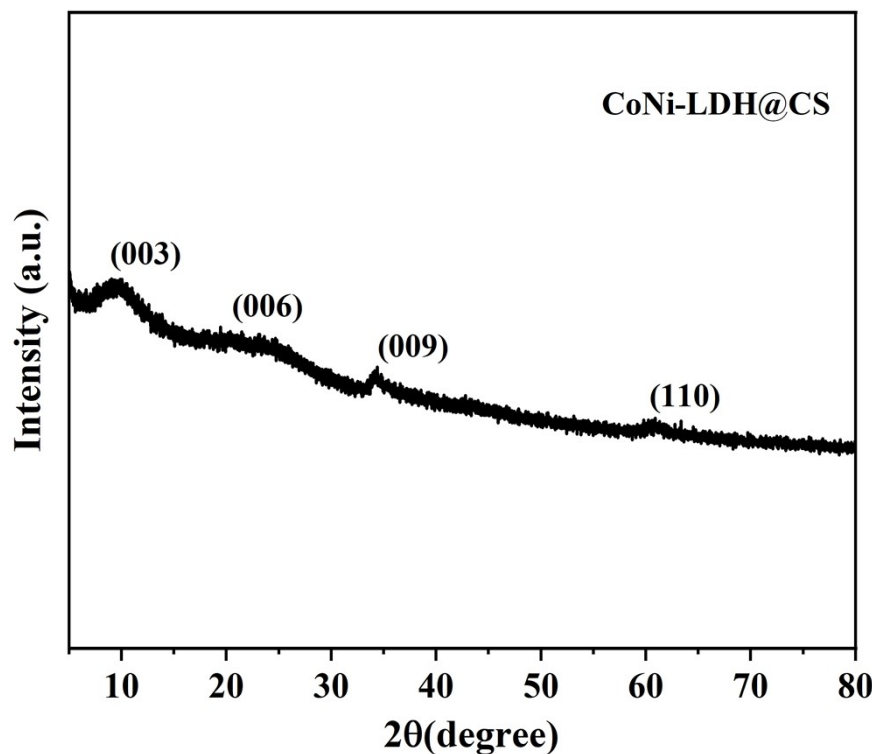


Fig. S1 The XRD pattern of CoNi-LDH@CS.

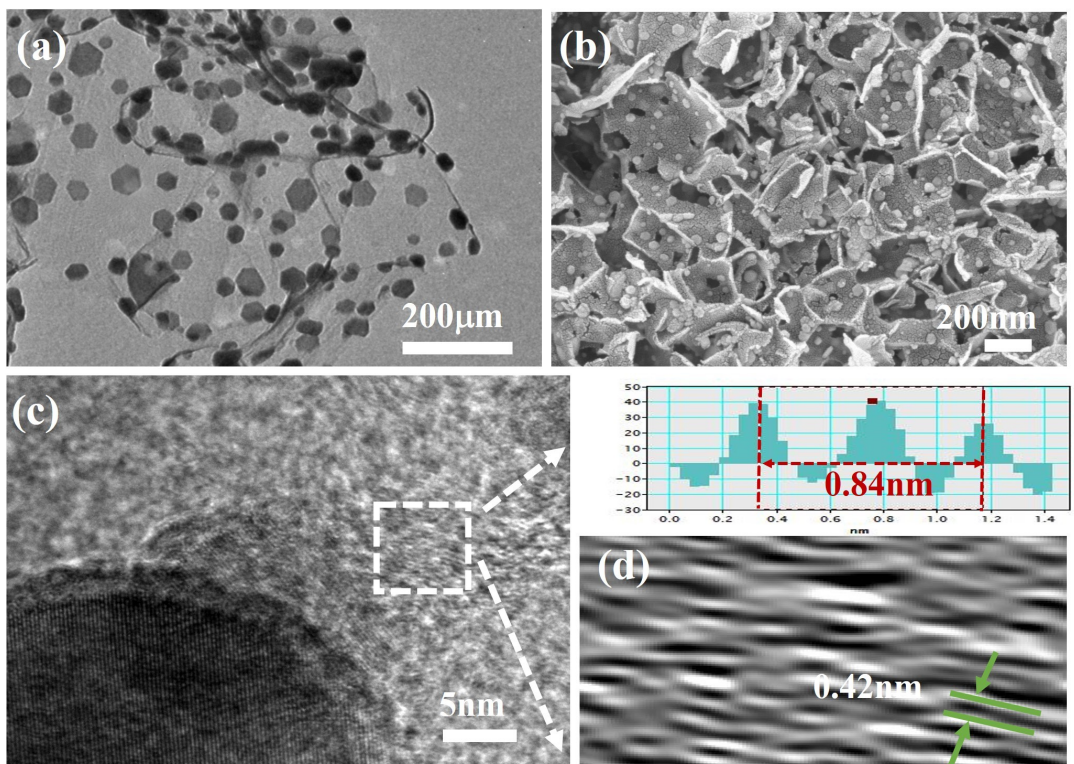


Fig. S2 (a-b) TEM and SEM images of $\text{Co}_{0.5}\text{Ni}_{0.5}\text{Te}_2@\text{CS}$. (c-d) HRTEM image of $\text{Co}_{0.5}\text{Ni}_{0.5}\text{Te}_2@\text{CS}$ and lattice fringes of CS.

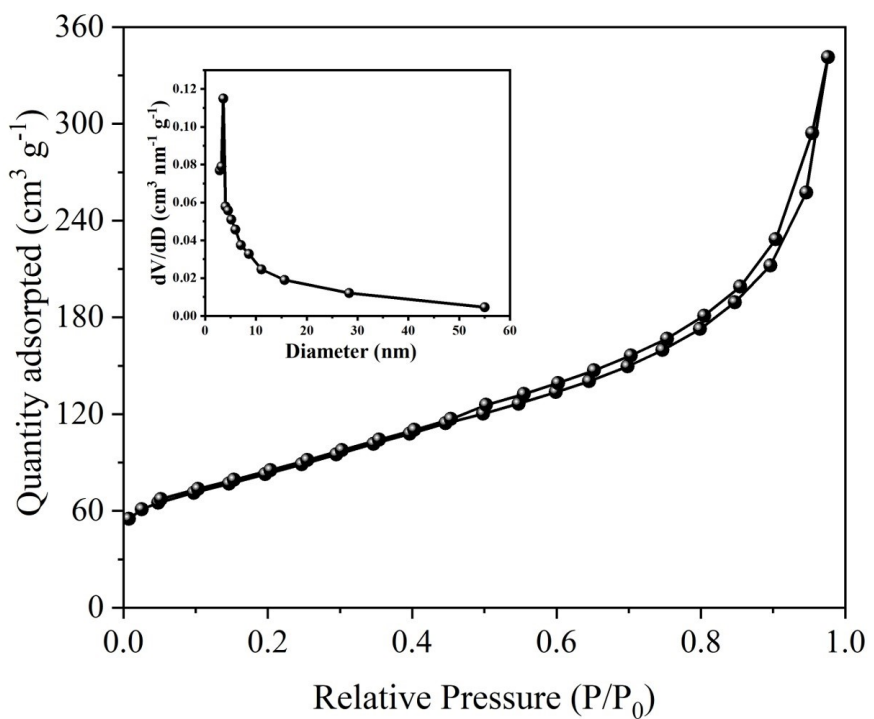


Fig. S3 N₂ adsorption-desorption isotherm and pore size distribution (inset) of CS.

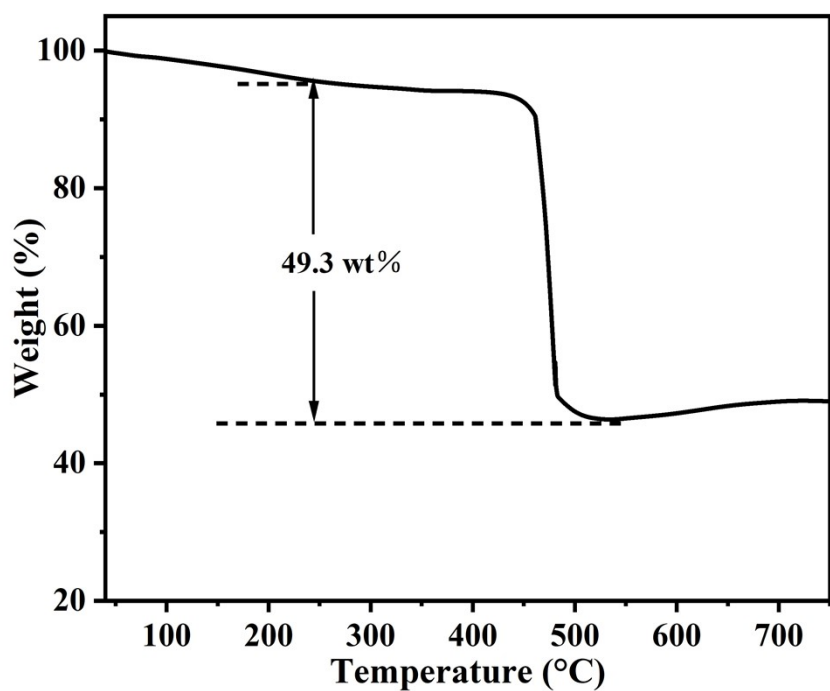


Fig. S4 TGA curve of $\text{Co}_{0.5}\text{Ni}_{0.5}\text{Te}_2@\text{CS}$.

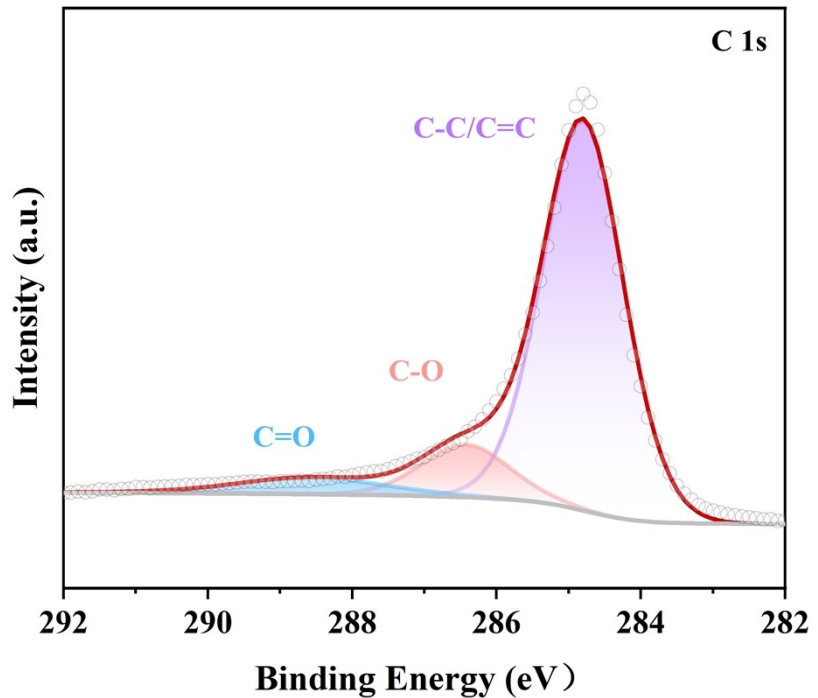


Fig. S5 XPS spectra of C1s.

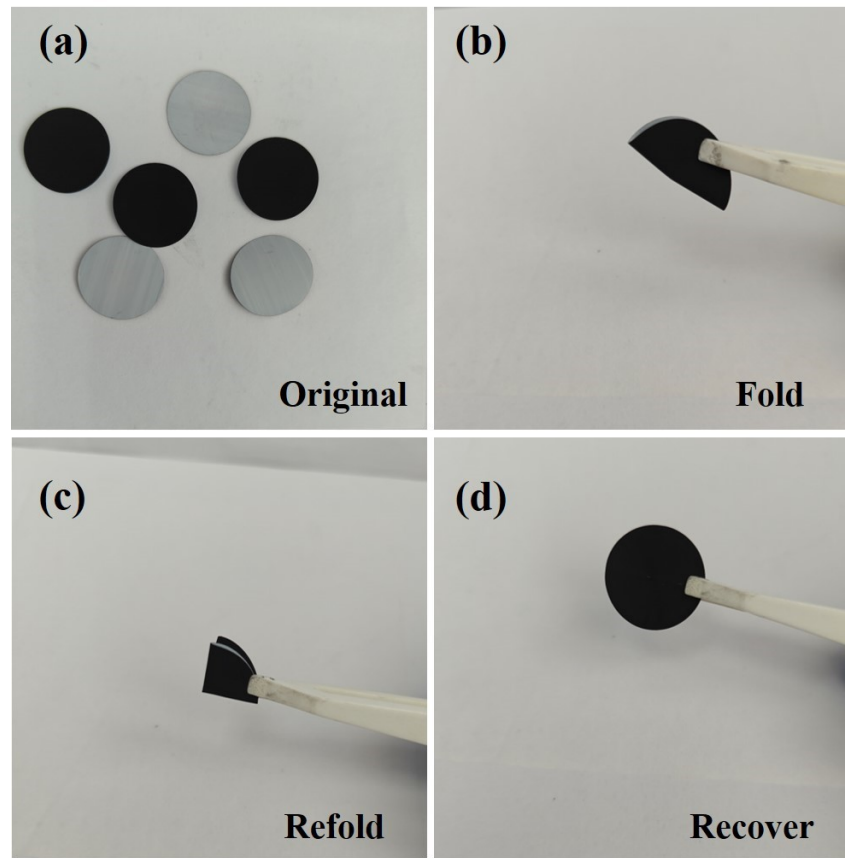


Fig. S6 The visual pictures of modified separator with $\text{Co}_{0.5}\text{Ni}_{0.5}\text{Te}_2@\text{CS}$ as coating layer (a) the original state, (b-c) folding and refolding state, (d) recovering state.

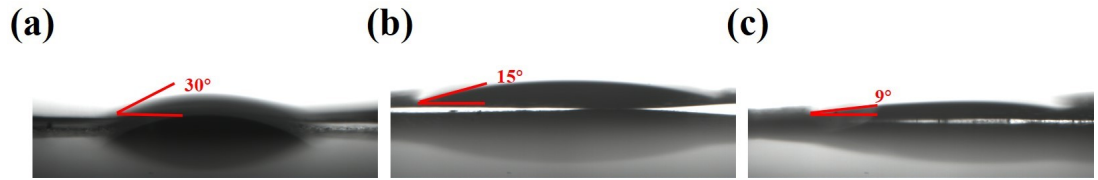


Fig. S7 The contact angles between electrolyte and (a) PP, (b) CS/PP and (c) Co_{0.5}Ni_{0.5}Te₂@CS/PP.

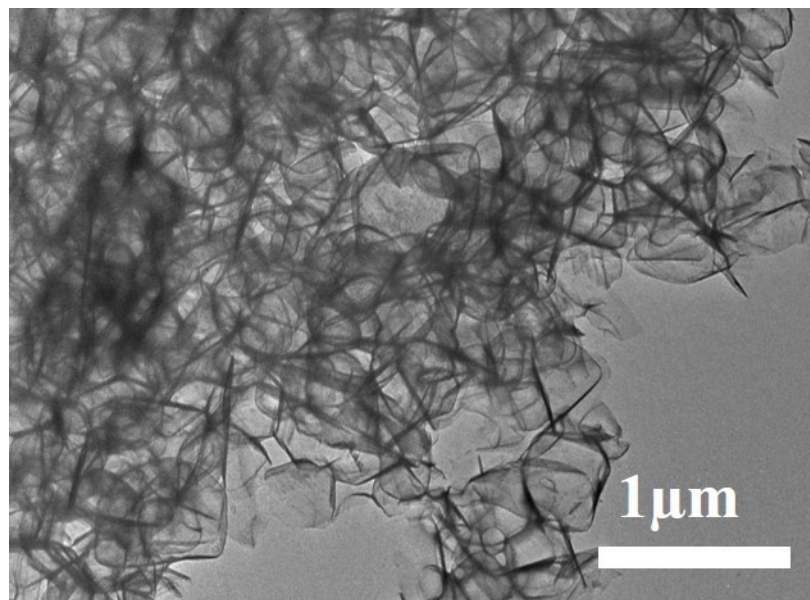


Fig. S8 TEM images of NPCS

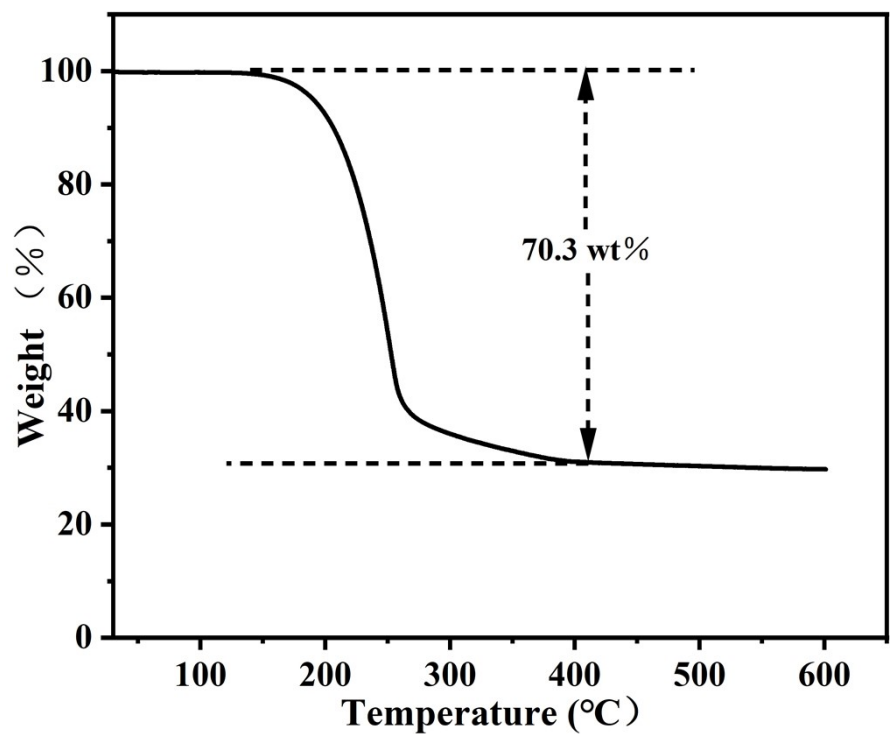


Fig. S9 TGA curve of S/NPCS.

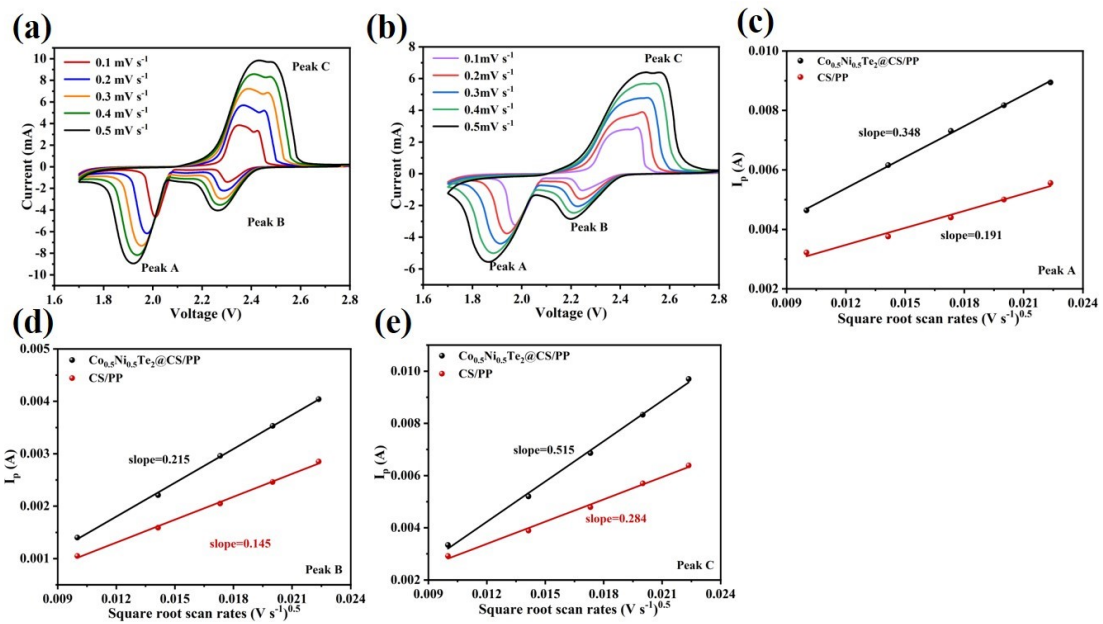


Fig. S10 CV profiles of cell with $\text{Co}_{0.5}\text{Ni}_{0.5}\text{Te}_2@\text{CS/PP}$ (a) and CS/PP (b) at various scan rates of $0.1\text{-}0.5 \text{ mV s}^{-1}$ and (c-e) the linear fitting curves of $I_p\text{-}v^{0.5}$ at peak A, B and C for cells with $\text{Co}_{0.5}\text{Ni}_{0.5}\text{Te}_2@\text{CS/PP}$ and CS/PP.

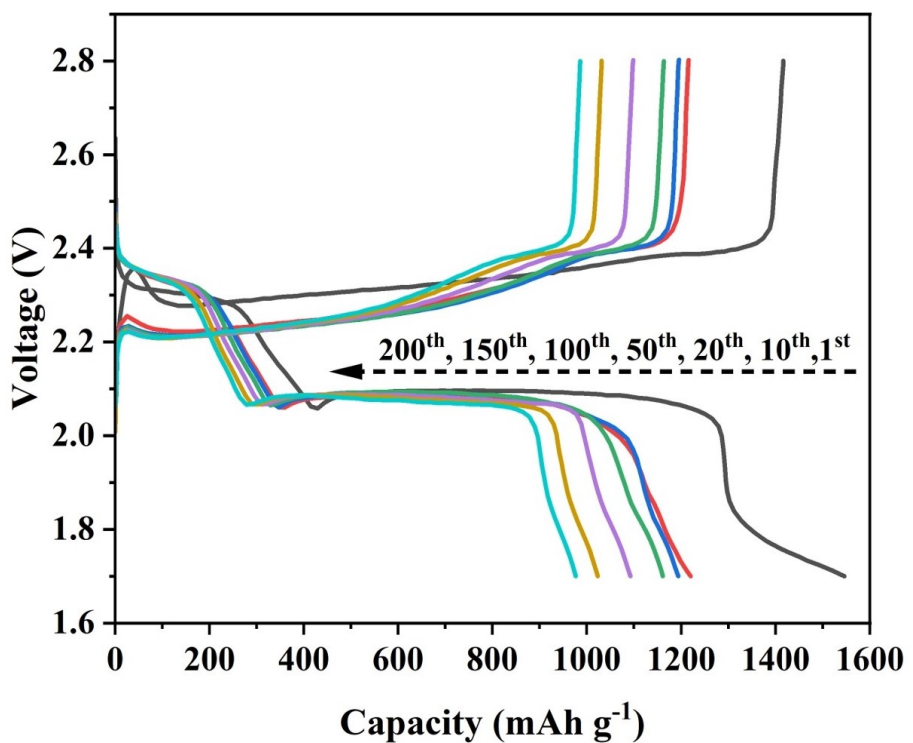


Fig. S11 The galvanostatic charge/discharge profiles of $\text{S}/\text//\text{Co}_{0.5}\text{Ni}_{0.5}\text{Te}_2@\text{CS/PP}$ with different cycles at 0.5 C.

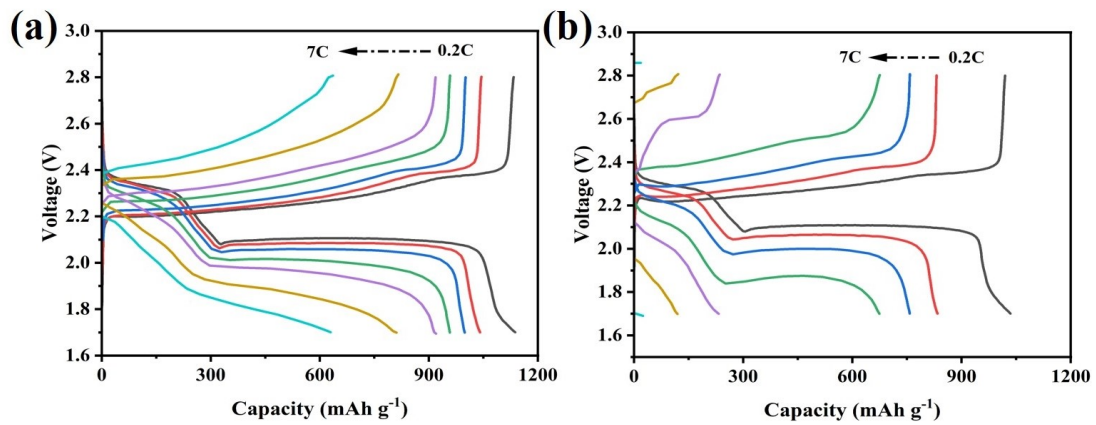


Fig. S12 The discharge-charge profiles at various rates ranged from 0.2 to 7 C:

(a) S//CS/PP and (b) S//PP.

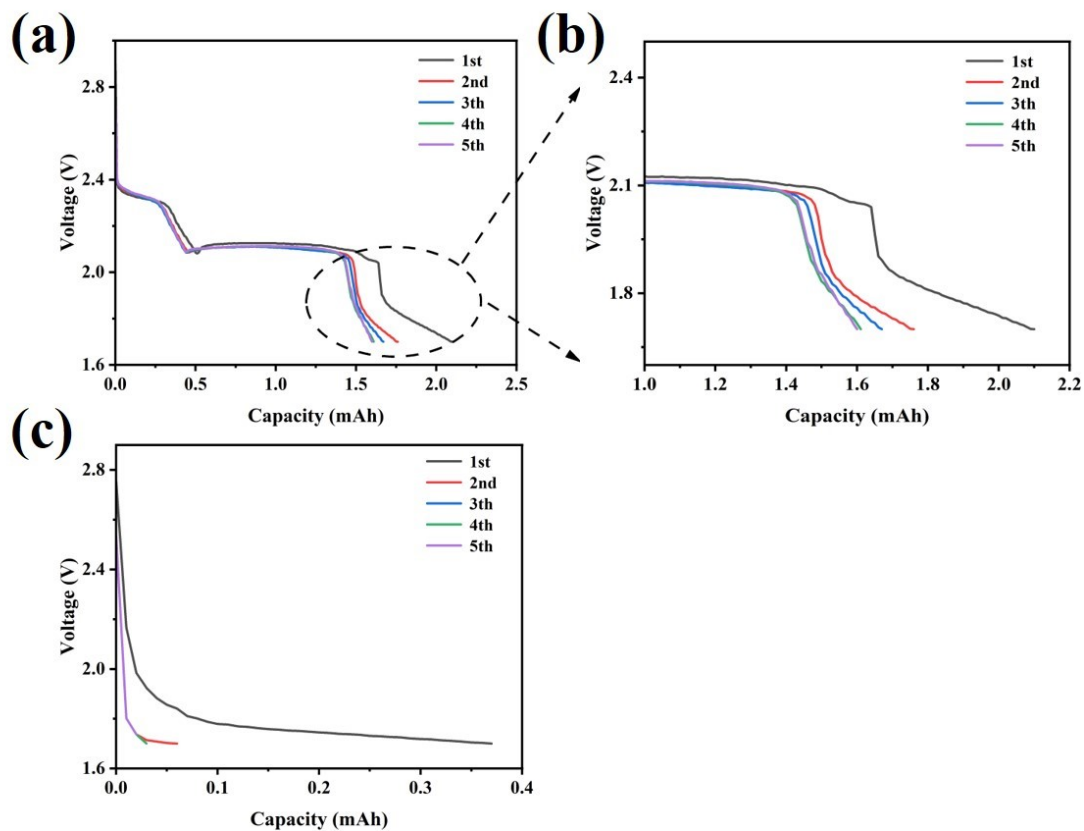


Fig. S13 (a-b) The voltage profiles of the cell with S//Co_{0.5}Ni_{0.5}Te₂@CS/PP at 0.2 C. (c) the voltage profiles of blank aluminum foil as electrode with Co_{0.5}Ni_{0.5}Te₂@CS/PP at 350 mA.

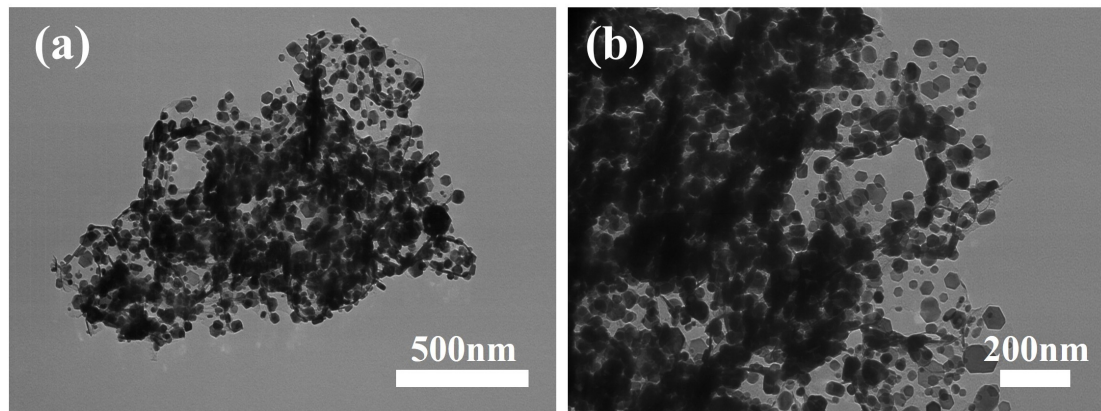


Fig. S14 TEM images of M-Co_{0.5}Ni_{0.5}Te₂@CS.

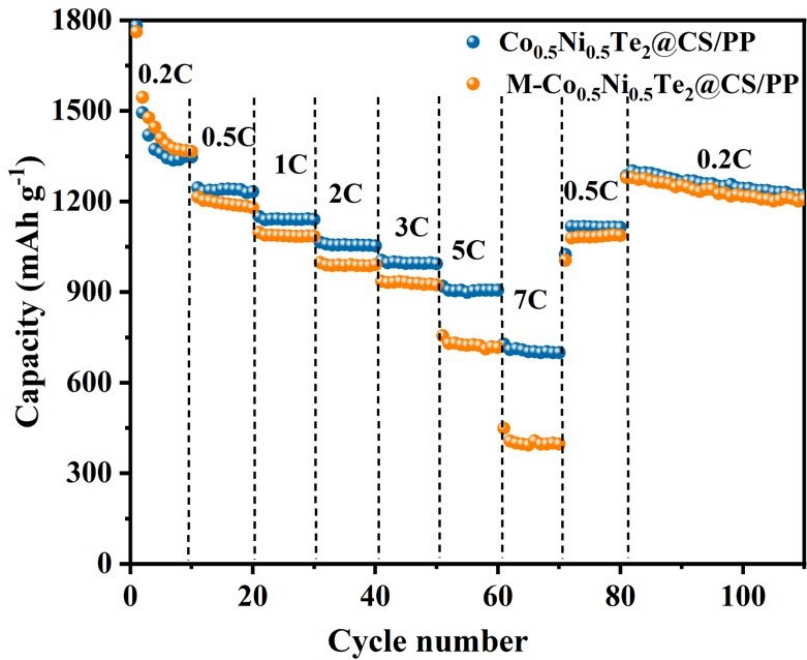


Fig. S15 the comparison of rate performance of cells with $\text{Co}_{0.5}\text{Ni}_{0.5}\text{Te}_2@\text{CS/PP}$ and $\text{M}-\text{Co}_{0.5}\text{Ni}_{0.5}\text{Te}_2@\text{CS/PP}$

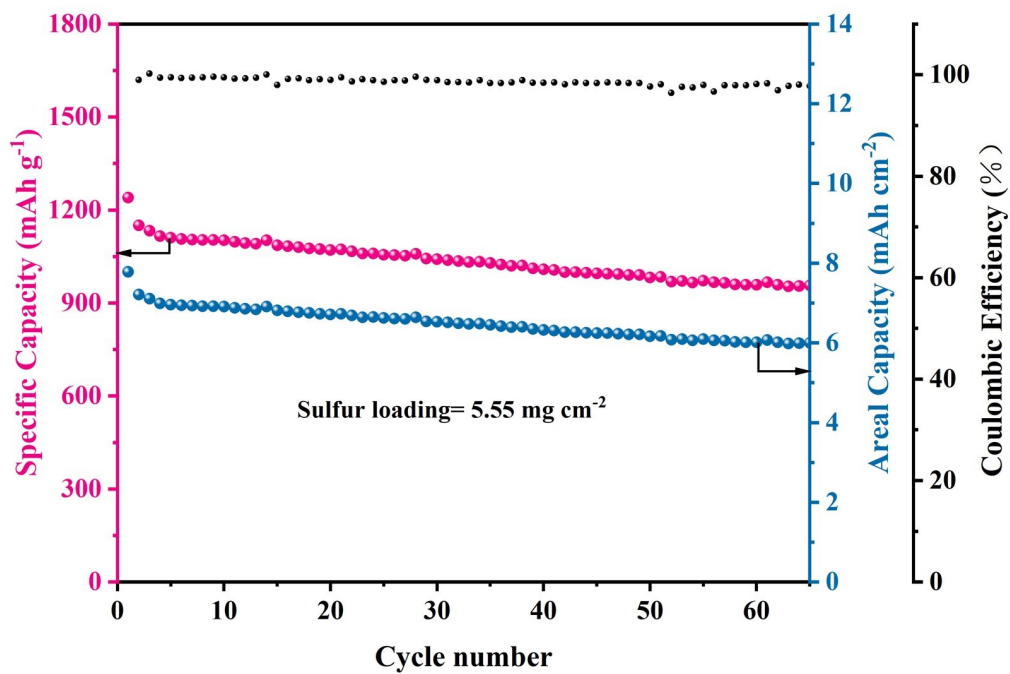


Fig. S16 The cycling stability of S// $\text{Co}_{0.5}\text{Ni}_{0.5}\text{Te}_2$ @CS/PP with sulfur loading of 5.55mg cm^{-2} .

Table S1. The values of Q1, Q2 and the ratios of Q2/Q1

	Q1 (mAh g ⁻¹)	Q2 (mAh g ⁻¹)	Q2/Q1
PP	306	663	2.16
CS/PP	323	737	2.28
Co _{0.5} Ni _{0.5} Te ₂ @CS/PP	360	934	2.59

Table S2. Comparison of Li-S battery performance assembled with different modified separators.

Separator Modifier	Loading (mg cm ⁻²)	C Rate	Cycle number	Capacity Retention (mAh g ⁻¹)	Ref
SV-VS ₂	0.50	0.2	150	921	[1]
NSPCF@CoS ₂	0.98	0.5	100	665	[2]
Oxygen-doped carbon/rGO	0.50	0.1	200	830	[3]
Ta ₄ C ₃ -Ta ₂ O ₅	0.81	1	500	457.1	[4]
TiB ₂ @Graphene	0.88	0.5	300	850	[5]
Fe ₃ O ₄ /RGO	0.60	0.3	200	563	[6]
Local 3D Co ₃ O ₄	0.43	2	300	548	[7]
NiCo ₂ O ₄ /CNF	2.00	2	500	658	[8]
Ni/PCMS	0.32	0.5	200	623.5	[9]
Ni/NiO-C	0.54	1	500	484	[10]
CoN@NCNT	0.54	0.2	200	729.7	[11]
PC/MWCNT	0.51	0.5	200	659	[12]
α -MnO ₂ @CNT	0.60	0.2	100	941	[13]
TiO ₂ @SCNT	0.34	0.5	200	848	[14]
Co@N-CNTs	0.64	1	500	610	[15]
NbN@NC	0.30	2	400	780.6	[16]
Co_{0.5}Ni_{0.5}Te₂@CS/PP	0.43	0.5	200	976.3	This work
		2	500	784.8	

References

1. L. He, X. Zhang, D. Yang, J. Li, M. Wang, S. Liu, J. Qiu, T. Ma, J. Ba, Y. Wang and Y. Wei, *Nano Lett.*, 2023, **23**, 7411-7418.
2. N. Wu, J. Wang, C. Liao, L. Han, L. Song, Y. Hu, X. Mu and Y. Kan, *J. Energy Chem.*, 2022, **64**, 372-384.
3. L. Zhang, F. Wan, X. Wang, H. Cao, X. Dai, Z. Niu, Y. Wang and J. Chen, *ACS Appl. Mater. Interfaces*, 2018, **10**, 5594-5602.
4. Q. Liang, S. Wang, X. Jia, J. Yang, Y. Li, D. Shao, L. Feng, J. Liao and H. Song, *Journal of Materials Science & Technology*, 2023, **151**, 89-98.
5. L. Jin, J. Ni, C. Shen, F. Peng, Q. Wu, D. Ye, J. Zheng, G. Li, C. Zhang, Z. Li and J. P. Zheng, *J. Power Sources*, 2020, **448**, 227336.
6. P. Cheng, P. Guo, D. Liu, Y. Wang, K. Sun, Y. Zhao and D. He, *J. Alloys Compd.*, 2019, **784**, 149-156.
7. L. Wu, C. Cai, X. Yu, Z. Chen, Y. Hu, F. Yu, S. Zhai, T. Mei, L. Yu and X. Wang, *ACS Appl. Mater. Interfaces*, 2022, **14**, 35894-35904.
8. J.-X. Lin, X.-M. Qu, X.-H. Wu, J. Peng, S.-Y. Zhou, J.-T. Li, Y. Zhou, Y.-X. Mo, M.-J. Ding, L. Huang and S.-G. Sun, *ACS Sustainable Chem. Eng.*, 2021, **9**, 1804-1813.
9. Z. Liu, C. Lu, S. Yuan, X. Ren and Y. Chen, *J. Alloys Compd.*, 2023, **960**, 170844.
10. J. Pu, T. Wang, X. Zhu, Y. Tan, L. Gao, J. Chen, J. Huang and Z. Wang, *Electrochim. Acta*, 2022, **435**, 141396.
11. H. Jia, J. Fan, P. Su, T. Guo and M.-C. Liu, *Small*, 2024, **20**, 2311343.
12. L. Tan, X. Li, Z. Wang, H. Guo, J. Wang and L. An, *ChemElectroChem*, 2018, **5**, 71-77.
13. J. Zu, W. Jing, X. Dai, Z. Feng, J. Sun, Q. Tan, Y. Chen and Y. Liu, *J. Alloys Compd.*, 2023, **933**, 167767.
14. Z. Gao, Z. Xue, Y. Miao, B. Chen, J. Xu, H. Shi, T. Tang and X. Zhao, *J. Alloys Compd.*, 2022, **906**, 164249.
15. G. Zhao, S. Liu, X. Zhang, Y. Zhang, H. Shi, Y. Liu, L. Hou and C. Yuan, *J. Mater. Chem. A*, 2023, **11**, 1856-1865.
16. N. Shi, B. Xi, J. Liu, Z. Zhang, N. Song, W. Chen, J. Feng and S. Xiong, *Adv. Funct. Mater.*, 2022, **32**, 2111586.